HHS Public Access

Author manuscript

Biochem Pharmacol. Author manuscript; available in PMC 2023 September 01.

Published in final edited form as:

Biochem Pharmacol. 2022 September ; 203: 115181. doi:10.1016/j.bcp.2022.115181.

A Newly Synthesized 17-epi-Neuroprotectin D1/17-epi-Protectin D1: Authentication and Functional Regulation of Inflammation-Resolution

Kajal Hamidzadeh[1], **Jodi Westcott**[2], **Nicholas Wourms**[2], **Ashley E. Shay**[1], **Anand Panigrahy**[1], **Michael J. Martin**[2], **Robert Nshimiyimana**[1], **Charles N. Serhan**[1,*]

[1]Center for Experimental Therapeutics and Reperfusion Injury, Department of Anesthesiology, Perioperative and Pain Medicine, Brigham and Women's Hospital and Harvard Medical School, Boston, Massachusetts 02115, USA

[2]Cayman Chemical Company, Ann Arbor, Michigan, USA

Abstract

The production of specialized pro-resolving mediators (SPMs) during the resolution phase in the inflammatory milieu is key to orchestrating the resolution of the acute inflammatory response. 17-epi-neuroprotectin D1/17-epi-protectin D1 (17-epi-NPD1/17-epi-PD1: 10*R*,17*R*-dihydroxy-4*Z*,7*Z*,11*E*,13*E*,15*Z*,19*Z*-docosahexaenoic acid) is an SPM of the protectin family, biosynthesized from docosahexaenoic acid (DHA), that exhibits both potent anti-inflammatory and neuroprotective functions. Here, we carried out a new commercial-scale synthesis of 17-epi-NPD1/17-epi-PD1 that enabled the authentication and confirmation of its potent bioactions *in vivo* and determination of its ability to activate human leukocyte phagocytosis. We provide evidence that this new synthetic 17-epi-NPD1/17-epi-PD1 statistically significantly increases human macrophage uptake of *E. coli in vitro* and confirm that it limits neutrophilic infiltration *in vivo* in a murine model of peritonitis. The physical properties of the new synthetic 17-epi-NPD1/17-epi-PD1, namely its ultra-violet absorbance, chromatography, and tandem mass spectrometry fragmentation pattern, matched those of the originally synthesized 17-epi-NPD1/17-epi-PD1. In addition, we verified the structure and complete stereochemical assignment of this new synthetic 17-epi-NPD1/17-epi-PD1 using nuclear magnetic resonance (NMR) spectroscopy.

[*]*Address correspondence to:* Prof. Charles N. Serhan, Director, Center for Experimental Therapeutics and Reperfusion Injury, Brigham and Women's Hospital, Hale Building for Transformative Medicine, 60 Fenwood Rd., 3-016, Boston, Massachusetts 02115, USA. Phone: 617-525-5001; Fax: 617-525-5017, cserhan@bwh.harvard.edu.

Kajal Hamidzadeh: Formal Analysis, Investigation, Writing-Original Draft, Writing-Review & Editing, Visualization. **Jodi Westcott:** Investigation, Resources, Formal Analysis. **Nicholas Wourms:** Investigation, Resources, Formal Analysis. **Ashley E. Shay:** Formal Analysis, Investigation, Visualization. **Anand Panigrahy:** Formal Analysis, Investigation, Visualization. **Michael J. Martin:** Investigation, Resources, Formal Analysis. **Robert Nshimiyimana**: Formal Analysis, Investigation, Writing-Original Draft, Writing-Review & Editing, Visualization. **Charles N. Serhan:** Conceptualization, Resources, Writing-Original Draft, Writing-Review & Editing, Supervision, Project administration, Funding Acquisition.

Conflict of Interest

The authors have no conflicts of interest to declare related to this report.

Together, these results authenticate this 17-epi-NPD1/17-epi-PD1 for its structure and potent pro-resolving functions.

Graphical Abstract

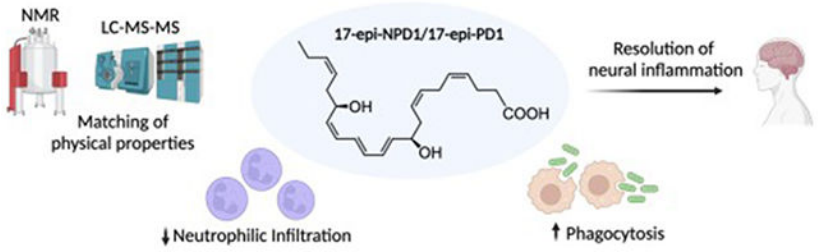

Keywords

lipid mediator; phagocytes; pro-resolving mediator; docosahexaenoic acid (DHA); neuroinflammation

1. Introduction

The COVID-19 pandemic and increases in cancer, as well as infection rates worldwide, have drawn attention to the critical role that excessive inflammation contributes to the pathologic basis of disease and organ failure [1]. Excessive inflammation can arise from the loss or deficiencies in endogenous resolution mediators and mechanisms [2]. The acute inflammatory response, while protective, if not completely resolved, can contribute to prolonged, excess inflammation. The pro-resolving mediators are endogenous molecules that are temporally biosynthesized by inflammatory exudates from essential polyunsaturated fatty acids, i.e., DHA, that limit neutrophil tissue infiltration and help clear apoptotic cells and microbes [2]. Among this new superfamily of pro-resolving mediators [3, 4] are the protectins [for review, see ref. 5]. First uncovered in the self-resolving inflammatory exudates [6] and biosynthesized from n-3 DHA in mice, this potent molecule protects human retinal pigment epithelial cells from stress [7] and was thus coined neuroprotectin D1, a novel conjugated triene that is produced from native DHA.

The complete stereochemistry and biosynthesis in human leukocytes of NPD1/PD1 (10*R*,17*S*-dihydroxy-4*Z*,7*Z*,11*E*,13*E*,15*Z*,19*Z*-docosahexaenoic acid) was determined [8], and its potent pro-resolving actions were confirmed [9] with material prepared by total organic synthesis. Several independent total organic syntheses of NPD1/PD1 and related molecules are reported [10–14].

NPD1/PD1 is produced by several other mammalian immune cell types, i.e. neutrophils, eosinophils [15], macrophages [16], and neural cells and tissues [17]. The pro-resolving functions of NPD1/PD1 extend to neural plasticity and reducing pain via TRPV1 [18], reducing skin inflammation [19], protecting from hearing loss [20], and controlling virus-induced pathologies as with *Herpes simplex* [21]. Both NPD1/PD1 and its double deoxygenation isomer, PDX, improve the severity of influenza A virus [22, 23]. NPD1/PD1

stimulate regeneration in zebrafish [24]. NPD1/PD1 biosynthesis from DHA proceeds via formation of a novel 16(17)-epoxide-containing intermediate [8] that was confirmed using total organic synthesis of the 16(17)-epoxide intermediate [13] and is produced by diabetic macrophages in wound healing [16]. Also, isolated enzymes involved include 15-lipoxygenase-1 and/or 15-lipoxygenase-2 [25], which are confirmed in initiating the biosynthesis of NPD1/PD1. In addition to the 17*S*-hydroxy chirality of native NPD1/PD1, its 17*R*-epimer can also be produced with aspirin-triggered biosynthesis [26] or via acetylation of cyclooxygenase-2 by sphingosine kinase 1 as in Alzheimer's disease [27]. This 17*R*-epimer shares the potent actions of NPD1/PD1 [26] in resolving neural inflammation [28].

Here, we report a new commercial-scale total synthesis of 17-epi-NPD1/17-epi-PD1 and authenticate both its physical properties and its potent pro-resolving actions in limiting tissue infiltration of neutrophils *in vivo* and enhancing macrophage-mediated phagocytosis; thus, confirming the potent key responses that are hallmarks of the resolution of inflammation.

2. Materials and Methods

2.1 Human macrophage differentiation

Human apheresis leukoreduction collars devoid of platelets were obtained from deidentified, healthy human volunteers from the Boston Children's Hospital Blood Donor Center under the IRB protocol #1999P0001279 approved by the Mass General Brigham Institutional Review Board. Peripheral blood mononuclear cells (PBMC) were isolated via density-gradient centrifugation using Ficoll-Histopaque 1.077 g/mL (Sigma-Aldrich, St. Louis, MO, USA). Monocytes were adhered to tissue culture treated plates for 1 hour, and non-adherent cells were removed. Monocytes were differentiated into macrophages for 7 days in RPMI-1640 medium (Lonza, Walkersville, MD, USA) supplemented with 10% fetal bovine serum (Gibco, Life Technologies, Grand Island, NY, USA), 2 mM L-glutamine (Lonza), 100 U/mL penicillin-100 μg/mL streptomycin (Lonza), and 20 ng/mL granulocyte-macrophage colony-stimulating factor (Peprotech, Cranbury, NJ, USA). Medium containing growth factor was removed prior to *in vitro* experiments and replaced with PBS containing calcium and magnesium, $PBS^{+/+}$ (Corning, Manassas, VA, USA).

2.2 Macrophage phagocytosis of *E. coli*

Human monocyte-derived macrophages were plated onto chamber slides (50,000 cells/chamber) and allowed to adhere overnight. *E. coli* (O6:K2:H1) was cultured overnight in Luria-Bertani broth (Invitrogen, Waltham, MA, USA) and labeled using *Bac*Light™ Green (Molecular Probes, Life Technologies, Eugene, OR, USA). The 17-epi-NPD1/17-epi-PD1 in the present studies was prepared by total organic synthesis as outlined in the methods and results sections, 2.6 and 3, respectively, and is now commercially available (Cayman Chemical Company, Ann Arbor, MI, USA). This mediator or vehicle (0.036% ethanol/$PBS^{+/+}$; vol/vol) was added to macrophages for 15 minutes (37 °C, pH 6.8-7.4) prior to the addition of the *Bac*Light Green-labeled *E. coli* (50 bacteria:1 macrophage ratio, 2.5 x 10^6 CFU). The concentration of 17-epi-NPD1/17-epi-PD1 was selected based on the range of

published concentrations reported in [26]. For all reported experiments, chamber slides were kept at 37 °C and 5% CO_2 in a stage-top incubation system equipped with a gas mixer and temperature regulator (TOKAI HIT, Fujinomiya, Japan). Multi-point imaging was carried out at 10-minute intervals for a total of 2 hours using a Keyence BZ-9000 (BIOREVO, Osaka, Japan) inverted fluorescence microscope at 20X magnification. The intensity of green fluorescence and cell counts for each image were quantified using the BZ-II Analyzer software (Keyence, Itasca, IL, USA).

2.3 Mouse zymosan-induced peritonitis

Male, 6–8-week-old FVB mice (Taconic Biosciences, Germantown, NY, USA), weighing approximately 23 g, were anesthetized with isoflurane (Covetrus, Portland, ME, USA) and injected i.p. with 2 mg zymosan A BioParticles™ from *S. cerevisiae* (Invitrogen, Eugene, OR, USA) suspended in 500 μl saline. Immediately following, 100 ng, 10 ng, or 1 ng of 17-epi-NPD1/17-epi-PD1 methyl ester or vehicle (0.1% ethanol) were injected i.v. in 100 μl saline. The dose range of 17-epi-NPD1/17-epi-PD1 was selected for *in vivo* authentication based on earlier reported dose response relationships [26]. Mice were euthanized 6 hours later in accordance with Brigham and Women's Institutional Animal Care and Use Committee animal protocol #2016N000145, and peritoneal exudates were harvested by lavage in 5 mL of PBS. Total leukocyte counts were determined, and differential cell counts were obtained using flow cytometry (LSR II, BD Biosciences, Franklin Lakes, NJ, USA) and visually examined by cytospin preparations stained with Wright-Giemsa (Richard-Allan Scientific, Thermo Fisher, Kalamazoo, MI, USA). Antibody staining of exudate cells was performed by first blocking with α-CD16/CD32 (eBioscience, Life Technologies Corp, Carlsbad, CA, USA) followed by staining with CD45 PerCP-Cy5.5 (Biolegend, San Diego, CA, USA), CD11b PE (Invitrogen, Life Technologies Corp, Carlsbad, CA, USA), F4/80 APC (eBioscience), Ly6C FITC (Biolegend), and Ly6G APC-Cy7 (Biolegend). The PMN and monocyte populations were identified via surface marker staining: $CD45^+CD11b^+F4/80^-Ly6G^+$ or $CD45^+CD11b^+F4/80^-Ly6C^+$, respectively, and analyzed using FlowJo software version X (BD Biosciences, Ashland, OR, USA).

2.4 Toxicity panel with LDH

Male, 6–8-week-old FVB mice were injected i.v. with 100 ng of 17-epi-NPD1/17-epi-PD1 methyl ester or vehicle (0.1% ethanol) in 100 μl of sterile saline, and 24 hours later, blood was collected and allowed to clot at room temperature for 3 hours. Samples were spun at 2000 x g for 10 minutes and serum was transferred to a new tube and stored at −20 °C. Samples were sent for toxicology analysis (IDEXX BioAnalytics, North Grafton, MA, USA). The toxicology panel included the following analytes: ALP, AST, ALT, albumin, total bilirubin, total protein, globulin, conjugated bilirubin, ALB/GLOB ratio, LDH, and unconjugated bilirubin.

2.5 Targeted liquid chromatography tandem mass spectrometry

17-epi-NPD1/17-epi-PD1 authentication was accomplished using a 6500^+ triple quadrupole QTRAP mass spectrometer in low mass negative mode (Sciex, Framingham, MA, USA) equipped with an ExionLC (Shimadzu, Kyoto, Japan) and a Kinetex 2.6 μm Polar C18 100 Å, LC Column 100 x 3.0 mm (Phenomenex, Torrance, CA, USA). The targeted multiple

reaction monitoring (MRM) settings were as follows: Q1: 359.2 Da, Q3: 153.1 Da, dwell time: 51.740 msec, collision energy: −21 V, declustering potential: −40 V, collision cell exit potential: −12 V, and entrance potential: −10 V. For gradient, library search parameters, as well as MRM and enhanced product ion (EPI) settings, see [29]. Liquid chromatography-tandem mass spectrometry (LC-MS/MS) data were acquired with Analyst version 1.7.1 (Sciex). A custom metabololipidomics MS/MS spectral library was constructed from validated synthetic materials and authentic biologic materials using LibraryView version 1.4 (Sciex). LC-MS/MS data were analyzed and presented as screen captures using Sciex OS-Q version 1.7.0.36606.

2.6 Synthesis and NMR of prepared 17-epi-NPD1/17-epi-PD1

Two key fragments prepared from commercially available building blocks were combined to yield the core structure of 17-epi-NPD1/17-epi-PD1 in a convergent manner [30]. A Boland reduction followed by alkaline hydrolysis afforded the target compound. ^{1}H and 2-dimensional correlated spectroscopy (COSY) data were acquired using a JEOL ECZ-400S spectrometer equipped with a 5 mm ROYALPROBE™ HFX probe at a field strength of 399.58 MHz. ^{1}H data were acquired with 256 transients, 14985 points, and a 2 s relaxation delay. COSY data were acquired with double-quantum filtering (DQF-COSY) with 4 transients, 1280 points in the X dimension, 256 points in the Y dimension, and a 1.5-second relaxation delay. Both spectra were acquired in methanol-d_4 at the ambient room temperature of 20.1°C. List of multiplicities: ^{1}H NMR (400 MHz, Methanol-d_4) δ 6.52 (dd, 1H, J=12.1, 13.5 Hz), 6.2–6.4 (m, 2H), 6.08 (t, 1H, J=11.2 Hz), 5.75 (dd, 1H, J=6.5, 14.5 Hz), 5.2–5.6 (m, 7H), 4.5–4.6 (m, 1H), 4.1–4.2 (m, 1H), 2.7–2.9 (m, 2H), 2.3–2.4 (m, 7H), 2.20 (td, 1H, J=7.0, 14.1 Hz), 2.07 (quin, 2H, J=7.3 Hz), 0.97 (t, 3H, J=7.5 Hz).

2.7 Statistical analysis

Two-tailed Student's t tests (unpaired or paired) were performed for comparisons between 2 groups using Prism software version 9.2.0 (GraphPad, San Diego, CA, USA). One-way ANOVA and Dunnett's test for multiple comparisons were performed for comparisons between the means of 3 or more groups. The P-values ≤ 0.05 were taken as statistically significant.

3. Results

The proposed biosynthesis of 17-epi-NPD1/17-epi-PD1 is illustrated in Figure 1A. The biosynthesis of NPD1/PD1 involves the conversion of docosahexaenoic acid (DHA) by 15-lipoxygenase [31] to the 17-hydroperoxy product depicted in Figure 1A, which is rapidly converted to an epoxide-containing intermediate, coined e-protectin (16*S*,17*S*-epoxy-protectin), that has been confirmed by total organic synthesis [8, 32]. This e-protectin is converted enzymatically to NPD1/PD1 by human phagocytes [32]. The complete stereochemistry and bioactions of NPD1/PD1 were confirmed using a total organic synthesis approach with stereoselective synthesis of NPD1/PD1 and related isomers that are produced via non-enzymatic hydrolysis of the 16*S*,17*S*-epoxy-protectin [8]. This approach was also carried out for the aspirin-triggered epimer produced via modified COX-2 [26]; see Figure 1A illustration and corresponding legend. The total synthesis of 17-epi-NPD1/17-epi-PD1

was accomplished using a convergent and stereocontrolled strategy (Figure 1B). A C_1-C_{14} vinyl iodide was synthesized in 14 steps from 3-bromo-1-propanol and S-glycidol building blocks. The cross coupling between this piece and a C_{15}-C_{22} fragment, built in 8 steps from *S*-glycidol, was achieved under Sonogashira conditions. The final steps involved a Zn(Cu/Ag) reduction and methyl ester hydrolysis to create 17-epi-NPD1/17-epi-PD1 [30].

3.1 The 17-epi-NPD1/17-epi-PD1 increases human macrophage phagocytosis

In order to authenticate the newly synthesized 17-epi-NPD1/17-epi-PD1, we next assessed its biological actions with human macrophages. The capture and clearance of pathogens and foreign particulates via phagocytosis is an essential function of macrophages in the maintenance of homeostasis [33]. Pro-resolving mediators, such as NPD1/PD1, potently enhance the uptake of both microbial and inert particles [9].

In the experiments reported in Figure 2, human macrophages were incubated with the new synthetic 17-epi-NPD1/17-epi-PD1 [10 pM] or exposed to vehicle (0.036% ethanol/$PBS^{+/+}$; vol/vol) for direct comparisons, 15 minutes before the addition of fluorescently labeled *E. coli* (50:1 ratio). Time-lapse imaging revealed that 17-epi-NPD1/17-epi-PD1 significantly increased the uptake of *E. coli* in a sustained manner, monitored for 2 hours (Figure 2A). The initial rate of bacterial internalization and linear regression from 0-30 minutes was approximately 2.26 times higher for macrophages exposed to 17-epi-NPD1/17-epi-PD1 relative to macrophages that received bacteria alone. Images of fluorescent *E. coli* inside treated and un-treated macrophages at 60 minutes are shown in Figure 2B. At this timepoint (60 minutes), this new synthetic 17-epi-NPD1/17-epi-PD1 augmented macrophage phagocytosis with a significant increase of approximately 61% at 10 pM compared to cells exposed to vehicle alone. These results demonstrate that the newly synthesized 17-epi-NPD1/17-epi-PD1 has potent activity with human macrophages, increasing their phagocytic rate (Figure 2). Therefore, the present results with the 17-epimer of NPD1/PD1 are consistent with those obtained earlier [26], documenting the potent actions of NPD1/PD1 with human phagocytes.

3.2 The newly synthesized 17-epi-NPD1/17-epi-PD1 limits neutrophilic infiltration *in vivo*

17-epi-NPD1/17-epi-PD1 was originally shown to limit the infiltration of neutrophils into the peritoneal cavity during peritonitis [26]. Thus, we next sought evidence for this biological action for the newly synthesized 17-epi-NPD1/17-epi-PD1 with leukocyte infiltration to the mouse peritoneum. Peritonitis was initiated with an injection of 2 mg zymosan A particles from *S. cerevisiae* into the peritoneum. This was immediately followed by the intravenous injection of either 100 ng, 10 ng, or 1 ng of 17-epi-NPD1/17-epi-PD1 methyl ester or vehicle alone. At 6 hours after the initiation of peritonitis, the mice were sacrificed, and peritoneal lavages were obtained. The cellular composition of the exudates was next determined by flow cytometry (Figure 3A). Newly synthesized 17-epi-NPD1/17-epi-PD1 significantly reduced total leukocyte counts in the exudates at each of the three doses tested compared to zymosan plus vehicle alone (Figure 3B). The new synthetic 17-epi-NPD1/17-epi-PD1 most significantly decreased the number of neutrophils in the peritoneum by approximately 72% on average at the 10 ng dose compared to zymosan plus vehicle (Figure 3C). The number of monocytes in the exudates was also decreased by the

new 17-epi-NPD1/17-epi-PD1 at each of the three doses tested (Figure 3D). These results confirm the biological actions of this newly synthesized 17-epi-NPD1/17-epi-PD1 in an *in vivo* model of acute inflammation and demonstrate that intravenous delivery of the new synthetic compound is effective in limiting leukocyte numbers in the peritoneum.

In order to assess whether the newly synthesized compound displayed any toxicity, mice were injected i.v. with 100 ng of 17-epi-NPD1/17-epi-PD1 methyl ester or vehicle (0.1% ethanol). At 24 hours later, serum was obtained for analysis of a commercial panel of toxicology markers (Table 1). No statistically significant differences were obtained between vehicle control or 17-epi-NPD1/17-epi-PD1 for any of the markers measured in the panel, which included ALP, AST, ALT, albumin, total bilirubin, total protein, globulin, conjugated bilirubin, ALB/GLOB ratio, LDH, and unconjugated bilirubin. These values were consistent with those reported in male, reference FVB mice [34].

3.3 Matching physical properties of the newly synthesized 17-epi-NPD1/17-epi-PD1

The total organic synthesis employed chiral pool-based strategy to install stereogenic centers from glycidol derivatives in conjunction with stereocontrolled transforms to secure the *Z/E* geometry. The stereochemical purity of the target material was validated via assignment of the double-bond geometry using two-dimensional correlation spectroscopy (COSY) ^{1}H-^{1}H NMR (Figure 4A). The purple plot depicts positive contours of cross peaks along the diagonal axis, allowing detailed olefinic and full proton interpretation of 17-epi-NPD1/17-epi-PD1 (Figures 4A and 4B).

In order to further authenticate this new synthetic 17-epi-NPD1/17-epi-PD1, we determined its physical characteristics for a direct comparison with the original synthetic 17-epi-NPD1/17-epi-PD1 [14, 26]. The distinctive triplet band of ultra-violet absorption obtained with 17-epi-NPD1/17-epi-PD1 gave a λ_{max}^{MeOH} at 270 nm and shoulders at 261 nm and 281 nm, confirming the presence of a conjugated triene chromophore (Figure 5A). Targeted liquid chromatography was carried out with the new and original synthetic 17-epi-NPD1/17-epi-PD1 as well as a co-injection of both compounds. Figure 5B shows results indicating that the new and original synthetic 17-epi-NPD1/17-epi-PD1 co-eluted at T_R = 12.75 minutes as a single peak. Tandem mass spectrometry of the new 17-epi-NPD1/17-epi-PD1 matched to the original 17-epi-NPD1/17-epi-PD1 (Figure 5C, **lower panel, grey**) in our custom library containing 215 individual MS/MS spectra for reference mediators, prepared in Sciex software (see Methods), gave an unbiased fit score of 99.6%. In agreement with the reference, this newly synthesized 17-epi-NPD1/17-epi-PD1 displayed a parent mass ion at *m/z* 359 = M-H and daughter ions including *m/z* 341 = M-H-H_2O, *m/z* 315 = M-H-CO_2, *m/z* 297 = M-H-H_2O-CO_2, *m/z* 279 = M-H-2H_2O-CO_2, *m/z* 261, *m/z* 243 = 261-H_2O, *m/z* 217 = 261-CO_2, *m/z* 188 = 206-H_2O, *m/z* 177, *m/z* 153, and *m/z* 119 = 181-H_2O-CO_2 (Figure 5C, **upper panel, blue**). Together, these results confirm that the physical properties of the newly synthesized 17-epi-NPD1/17-epi-PD1 match those of our in-house, authentic 17-epi-NPD1/17-epi-PD1.

4. Discussion

In the present manuscript, we report the authentication of the newly synthesized 17-epi-neuroprotectin D1/17-epi-protectin D1. These results provide an additional confirmation of both the physical properties of 17-epi-NPD1/17-epi-PD1 and its potent functions in key cellular mechanisms and responses of interest in the resolution of inflammation. These include limiting further neutrophil infiltration, as directly determined in zymosan-stimulated peritonitis *in vivo* with mice (Figure 3) and stimulating bacterial phagocytosis by human macrophages (Figure 2). Together the present results provide an additional confirmation of the earlier physical and biological properties of the novel 17-epi-NPD1/17-epi-PD1, a member of the protectin family [26], and further establish the potent *in vivo* actions of this 17-epimer of NPD1/PD1.

Of interest, endogenous 17-epi-NPD1/17-epi-PD1 is present in human breast milk [35], in periodontal inflammation [36], and in human cerebrospinal fluid from older adults after surgery [37]. NPD1/PD1 is present and reduced in the cerebrospinal fluid of patients with Alzheimer's disease [38]. Human vagus nerve stimulation leads to local 17-epi-NPD1/17-epi-PD1 production along with several other DHA-derived pro-resolving mediators [39]. With this new source of 17-epi-NPD1/17-epi-PD1 available, it is likely that additional reports on the identification and *in vivo* actions will sharply increase and expand our knowledge of the role of this endogenous mediator in human physiology and pathology.

Along these lines, NPD1/PD1 protects from postoperative delirium behavior in aged mice [28], and intranasal administration of NPD1/PD1 along with other pro-resolving mediators (RvE1, RvD1, RvD2, MaR1) reduced neural inflammation and thus restored memory in an Alzheimer's mouse model [40]. These are functions that will very likely be shared by 17-epi-NPD1/17-epi-PD1 because this 17*R*-epimer will be locally inactivated more slowly *in vivo* by delaying dehydrogenation at the carbon-17 position similar to the Resolvin E1 analog [41]. 17-epi-NPD1/17-epi-PD1 is effective in experimental stroke [42]. Elegant studies by Balas *et al.* [43] indicate that NPD1/PD1 is rapidly metabolized locally via beta-oxidation. Drugs such as dexamethasone, used to treat COVID-19 infections in humans, stimulate NPD1/PD1 production *in vivo* in the lung tissues and can evoke resolution of inflammation in experimental animal models of disease [44]. GPR37 has been identified as a receptor for NPD1/PD1, mediating its ability to reduce pain and induce macrophage phagocytosis [45] and increase survival in sepsis models [46]. It is possible that the bioactions of 17-epi-NPD1/17-epi-PD1 share this receptor. Stable analog mimetics of NPD1/PD1 show remarkably potent properties *in vivo* [12] reducing neuropathic pain and chronic itch as in [11]. Thus, it will be exciting to determine whether 17-epi-NPD1/17-epi-PD1 mimetic analogs also carry these potent actions for these unmet medical needs and whether 17-epi-NPD1/17-epi-PD1, as demonstrated herein, can exhibit properties suitable for it to enter human clinical trials in the near future to stimulate the body's own resolution response circuit in settings of excess, uncontrolled inflammation.

Acknowledgements

We thank Mary H. Small for expert assistance in manuscript preparation. CNS's research is supported by National Institutes of Health USA (grant numbers R01GM38765 and R35GM139430).

Abbreviations

17-epi-NPD1/17-epi-PD1
10*R*, 17*R*-dihydroxy-4*Z*,7*Z*,11*E*,13*E*,15*Z*,19*Z*-docosahexaenoic acid

NPD1/PD1
10*R*,17*S*-dihydroxy-4*Z*,7*Z*,11*E*,13*E*,15*Z*,19*Z*-docosahexaenoic acid

17-H(p)DHA
17-hydro(peroxy)-4*Z*,7*Z*,10*Z*,13*Z*,15*E*,19*Z*-docosahexaenoic Acid

17-epi-H(p)DHA
17*R*-hydro(peroxy)-4*Z*,7*Z*,10*Z*,13*Z*,15*E*,19*Z*-docosahexaenoic acid

16*S*,17*S*-epoxy-protectin
16*S*,17*S*-epoxy-4*Z*,7*Z*,10*Z*,12*E*,14*E*,19*Z*-docosahexaenoic acid; e-protectin

DHA
4*Z*,7*Z*,10*Z*,13*Z*,16*Z*,19*Z*-docosahexaenoic acid

SPM
specialized pro-resolving mediator

15-LOX
15-lipoxygenase

COX-2
cyclooxygenase-2

PMN
polymorphonuclear cell

PBMC
peripheral blood mononuclear cells

MRM
multiple reaction monitoring

COSY
correlated spectroscopy

NMR
nuclear magnetic resonance

LC-MS/MS
liquid chromatography tandem mass spectrometry

E. coli
Escherichia coli (serotype O6:K2:H1)

S. cerevisiae

Saccharomyces cerevisiae

References

[1]. Daniels NF, Burrin C, Chan T, Fusco F, A Systematic Review of the Impact of the First Year of COVID-19 on Obesity Risk Factors: A Pandemic Fueling a Pandemic?, Curr Dev Nutr 6(4) (2022) nzac011. [PubMed: 35415391]

[2]. Serhan CN, Pro-resolving lipid mediators are leads for resolution physiology, Nature 510(7503) (2014) 92–101. [PubMed: 24899309]

[3]. Haeggstrom JZ, Leukotriene biosynthetic enzymes as therapeutic targets, J. Clin. Invest 128(7) (2018) 2680–2690. [PubMed: 30108195]

[4]. Serhan CN, Levy BD, Resolvins in inflammation: emergence of the pro-resolving superfamily of mediators, J. Clin. Invest 128 (2018) 2657–2669. [PubMed: 29757195]

[5]. Serhan CN, Dalli J, Colas RA, Winkler JW, Chiang N, Protectins and maresins: New pro-resolving families of mediators in acute inflammation and resolution bioactive metabolome, Biochim. Biophys. Acta 1851 (2015) 397–413. [PubMed: 25139562]

[6]. Serhan CN, Hong S, Gronert K, Colgan SP, Devchand PR, Mirick G, Moussignac R-L, Resolvins: a family of bioactive products of omega-3 fatty acid transformation circuits initiated by aspirin treatment that counter pro-inflammation signals, J. Exp. Med 196 (2002) 1025–1037. [PubMed: 12391014]

[7]. Mukherjee PK, Marcheselli VL, Serhan CN, Bazan NG, Neuroprotectin D1: a docosahexaenoic acid-derived docosatriene protects human retinal pigment epithelial cells from oxidative stress, Proc. Natl. Acad. Sci. U.S.A 101 (2004) 8491–8496. [PubMed: 15152078]

[8]. Serhan CN, Gotlinger K, Hong S, Lu Y, Siegelman J, Baer T, Yang R, Colgan SP, Petasis NA, Anti-inflammatory actions of neuroprotectin D1/protectin D1 and its natural stereoisomers: assignments of dihydroxy-containing docosatrienes, J. Immunol 176 (2006) 1848–1859. [PubMed: 16424216]

[9]. Schwab JM, Chiang N, Arita M, Serhan CN, Resolvin E1 and protectin D1 activate inflammation-resolution programmes, Nature 447 (2007) 869–874. [PubMed: 17568749]

[10]. Balas L, Durand T, Dihydroxylated E E, Z-docosatrienes. An overview of their synthesis and biological significance, Prog. Lipid Res 61 (2016) 1–18. [PubMed: 26545300]

[11]. Nesman JI, Chen O, Luo X, Ji RR, Serhan CN, Hansen TV, A new synthetic protectin D1 analog 3-oxa-PD1(n-3 DPA) reduces neuropathic pain and chronic itch in mice, Org Biomol Chem 19(12) (2021) 2744–2752. [PubMed: 33687402]

[12]. Dayaker G, Durand T, Balas L, Total synthesis of neuroprotectin D1 analogues derived from omega-6 docosapentaenoic acid (DPA) and adrenic acid (AdA) from a common pivotal, late-stage intermediate, J. Org. Chem 79(6) (2014) 2657–65. [PubMed: 24571431]

[13]. Tungen JE, Aursnes M, Ramon S, Colas RA, Serhan CN, Olberg DE, Nuruddin S, Willoch F, Hansen TV, Synthesis of protectin D1 analogs: novel pro-resolution and radiotracer agents, Org Biomol Chem 16(36) (2018) 6818–6823. [PubMed: 30204204]

[14]. Petasis NA, Yang R, Winkler JW, Zhu M, Uddin J, Bazan NG, Serhan CN, Stereocontrolled total synthesis of neuroprotectin D1 / protectin D1 and its aspirin-triggered stereoisomer, Tetrahedron Lett. 53(14) (2012) 1695–1698. [PubMed: 22690022]

[15]. Miyata J, Fukunaga K, Iwamoto R, Isobe Y, Niimi K, Takamiya R, Takihara T, Tomomatsu K, Suzuki Y, Oguma T, Sayama K, Arai H, Betsuyaku T, Arita M, Asano K, Dysregulated synthesis of protectin D1 in eosinophils from patients with severe asthma, J. Allergy Clin. Immunol 131 (2013) 353–360. [PubMed: 23006546]

[16]. Hong S, Tian H, Lu Y, Laborde JM, Muhale FA, Wang Q, Alapure BV, Serhan CN, Bazan NG, Neuroprotectin/protectin D1: endogenous biosynthesis and actions on diabetic macrophages in promoting wound healing and innervation impaired by diabetes, Am J Physiol Cell Physiol 307(11) (2014) C1058–67. [PubMed: 25273880]

[17]. Lukiw WJ, Cui JG, Marcheselli VL, Bodker M, Botkjaer A, Gotlinger K, Serhan CN, Bazan NG, A role for docosahexaenoic acid-derived neuroprotectin D1 in neural cell survival and Alzheimer disease, J. Clin. Invest 115 (2005) 2774–2783. [PubMed: 16151530]

[18]. Park CK, Lü N, Xu ZZ, Liu T, Serhan CN, Ji RR, Resolving TRPV1 and TNF-α-mediated spinal cord synaptic plasticity and inflammatory pain with neuroprotectin D1, J. Neurosci 31 (2011) 15072–15085. [PubMed: 22016541]

[19]. Park KD, Kim N, Kang J, Dhakal H, Kim JY, Jang YH, Lee WJ, Lee SJ, Kim SH, Protectin D1 reduces imiquimod-induced psoriasiform skin inflammation, Int Immunopharmacol 98 (2021) 107883. [PubMed: 34153674]

[20]. Ríos JD, Hughes CK, Lally J, Wienandt N, Esquivel C, Serhan CN, Weitzel EK, Neuroprotectin D1 Attenuates Blast Overpressure Induced Reactive Microglial Cells in the Cochlea, Laryngoscope 131(6) (2021) E2018–e2025. [PubMed: 33427310]

[21]. Rajasagi NK, Reddy PB, Mulik S, Gjorstrup P, Rouse BT, Neuroprotectin D1 reduces the severity of herpes simplex virus-induced corneal immunopathology, Invest. Ophthalmol. Vis. Sci 54(9) (2013) 6269–79. [PubMed: 23942967]

[22]. Morita M, Kuba K, Ichikawa A, Nakayama M, Katahira J, Iwamoto R, Watanebe T, Sakabe S, Daidoji T, Nakamura S, Kadowaki A, Ohto T, Nakanishi H, Taguchi R, Nakaya T, Murakami M, Yoneda Y, Arai H, Kawaoka Y, Penninger JM, Arita M, Imai Y, The lipid mediator protectin D1 inhibits influenza virus replication and improves severe influenza, Cell 153 (2013) 112–125. [PubMed: 23477864]

[23]. Imai Y, Role of omega-3 PUFA-derived mediators, the protectins, in influenza virus infection, Biochim. Biophys. Acta 1851(4) (2015) 496–502. [PubMed: 25617737]

[24]. Nguyen-Chi M, Luz-Crawford P, Balas L, Sipka T, Contreras-López R, Barthelaix A, Lutfalla G, Durand T, Jorgensen C, Djouad F, Pro-resolving mediator protectin D1 promotes epimorphic regeneration by controlling immune cell function in vertebrates, Br. J. Pharmacol 177 (2020) 4055–4073. [PubMed: 32520398]

[25]. Tsai WC, Kalyanaraman C, Yamaguchi A, Holinstat M, Jacobson MP, Holman TR, In Vitro Biosynthetic Pathway Investigations of Neuroprotectin D1 (NPD1) and Protectin DX (PDX) by Human 12-Lipoxygenase, 15-Lipoxygenase-1, and 15-Lipoxygenase-2, Biochemistry 60(22) (2021) 1741–1754. [PubMed: 34029049]

[26]. Serhan CN, Fredman G, Yang R, Karamnov S, Belayev LS, Bazan NG, Zhu M, Winkler JW, Petasis NA, Novel proresolving aspirin-triggered DHA pathway, Chem. Biol 18 (2011) 976–987. [PubMed: 21867913]

[27]. Lee JY, Han SH, Park MH, Baek B, Song IS, Choi MK, Takuwa Y, Ryu H, Kim SH, He X, Schuchman EH, Bae JS, Jin HK, Neuronal SphK1 acetylates COX2 and contributes to pathogenesis in a model of Alzheimer's Disease, Nat Commun 9(1) (2018) 1479. [PubMed: 29662056]

[28]. Zhou Y, Wang J, Li X, Li K, Chen L, Zhang Z, Peng M, Neuroprotectin D1 Protects Against Postoperative Delirium-Like Behavior in Aged Mice, Front Aging Neurosci 12 (2020) 582674. [PubMed: 33250764]

[29]. Shay AE, Nshimiyimana R, Petasis NA, Haeggstrom JZ, Serhan CN, Human leukocytes selectively convert 4S,5S-epoxy-Resolvin to Resolvin D3, Resolvin D4, and a cys-Resolvin isomer, Proc. Natl. Acad. Sci. USA 118 (2021) e2116559118. [PubMed: 34911767]

[30]. Serhan CN, Petasis NA, Resolvins and protectins in inflammation-resolution, Chem. Rev 111 (2011) 5922–5943. [PubMed: 21766791]

[31]. Hong S, Gronert K, Devchand P, Moussignac R-L, Serhan CN, Novel docosatrienes and 17S-resolvins generated from docosahexaenoic acid in murine brain, human blood and glial cells: autacoids in anti-inflammation, J. Biol. Chem 278 (2003) 14677–14687. [PubMed: 12590139]

[32]. Aursnes M, Tungen JE, Colas RA, Vlasakov I, Dalli J, Serhan CN, Hansen TV, Synthesis of the 16S,17S-Epoxyprotectin Intermediate in the Biosynthesis of Protectins by Human Macrophages, J. Nat. Prod 78 (2015) 2924–2931. [PubMed: 26580578]

[33]. Cotran RS, Kumar V, Collins T, Robbins Pathologic Basis of Disease, W.B. Saunders Co., Philadelphia, 1999.

[34]. Schneck K, Washington M, Holder D, Lodge K, Motzel S, Hematologic and serum biochemical reference values in nontransgenic FVB mice, Comp Med 50(1) (2000) 32–5. [PubMed: 10987664]

[35]. Arnardottir H, Orr SK, Dalli J, Serhan CN, Human milk proresolving mediators stimulate resolution of acute inflammation, Mucosal Immunol. 9 (2016) 757–766. [PubMed: 26462421]

[36]. Ferguson B, Bokka NR, Maddipati KR, Ayilavarapu S, Weltman R, Zhu L, Chen W, Zheng WJ, Angelov N, Van Dyke TE, Lee CT, Distinct Profiles of Specialized Pro-resolving Lipid Mediators and Corresponding Receptor Gene Expression in Periodontal Inflammation, Front Immunol 11 (2020) 1307. [PubMed: 32670289]

[37]. Terrando N, Park JJ, Devinney M, Chan C, Cooter M, Avasarala P, Mathew JP, Quinones QJ, Maddipati KR, Berger M, Immunomodulatory lipid mediator profiling of cerebrospinal fluid following surgery in older adults, Sci Rep 11(1) (2021) 3047. [PubMed: 33542362]

[38]. Do KV, Hjorth E, Wang Y, Jun B, Kautzmann MI, Ohshima M, Eriksdotter M, Schultzberg M, Bazan NG, Cerebrospinal Fluid Profile of Lipid Mediators in Alzheimer's Disease, Cell. Mol. Neurobiol doi: 10.1007/s10571-022-01216-5 (2022).

[39]. Serhan CN, De la Rosa X, Jouvene CC, Cutting Edge: Human vagus produces specialized pro-resolving mediators of inflammation with electrical stimulation reducing pro-inflammatory eicosanoids, J. Immunol 201 (2018) 3161–3165. [PubMed: 30355784]

[40]. Emre C, Arroyo-García LE, Do KV, Jun B, Ohshima M, Alcalde SG, Cothern ML, Maioli S, Nilsson P, Hjorth E, Fisahn A, Bazan NG, Schultzberg M, Intranasal delivery of pro-resolving lipid mediators rescues memory and gamma oscillation impairment in App(NL-G-F/NL-G-F) mice, Commun Biol 5(1) (2022) 245. [PubMed: 35314851]

[41]. Arita M, Oh S, Chonan T, Hong S, Elangovan S, Sun Y-P, Uddin J, Petasis NA, Serhan CN, Metabolic inactivation of resolvin E1 and stabilization of its anti-inflammatory actions, J. Biol. Chem 281 (2006) 22847–22854. [PubMed: 16757471]

[42]. Bazan NG, Eady TN, Khoutorova L, Atkins KD, Hong S, Lu Y, Zhang C, Jun B, Obenaus A, Fredman G, Zhu M, Winkler JW, Petasis NA, Serhan CN, Belayev L, Novel aspirin-triggered neuroprotectin D1 attenuates cerebral ischemic injury after experimental stroke, Exp. Neurol 236(1) (2012) 122–30. [PubMed: 22542947]

[43]. Balas L, Risé P, Gandrath D, Rovati G, Bolego C, Stellari F, Trenti A, Buccellati C, Durand T, Sala A, Rapid Metabolization of Protectin D1 by β-Oxidation of Its Polar Head Chain, J. Med. Chem 62(21) (2019) 9961–9975. [PubMed: 31626541]

[44]. Andreakos E, Papadaki M, Serhan CN, Dexamethasone, pro-resolving lipid mediators and resolution of inflammation in COVID-19, Allergy 76(3) (2021) 626–628. [PubMed: 32956495]

[45]. Bang S, Xie YK, Zhang ZJ, Wang Z, Xu ZZ, Ji RR, GPR37 regulates macrophage phagocytosis and resolution of inflammatory pain, J. Clin. Invest 128(8) (2018) 3568–3582. [PubMed: 30010619]

[46]. Bang S, Donnelly CR, Luo X, Toro-Moreno M, Tao X, Wang Z, Chandra S, Bortsov AV, Derbyshire ER, Ji RR, Activation of GPR37 in macrophages confers protection against infection-induced sepsis and pain-like behaviour in mice, Nat Commun 12(1) (2021) 1704. [PubMed: 33731716]

[47]. Morello E, Pérez-Berezo T, Boisseau C, Baranek T, Guillon A, Bréa D, Lanotte P, Carpena X, Pietrancosta N, Hervé V, Ramphal R, Cenac N, Si-Tahar M, Pseudomonas aeruginosa Lipoxygenase LoxA Contributes to Lung Infection by Altering the Host Immune Lipid Signaling, Front Microbiol 10 (2019) 1826. [PubMed: 31474948]

[48]. Lucido MJ, Orlando BJ, Vecchio AJ, Malkowski MG, Crystal Structure of Aspirin-Acetylated Human Cyclooxygenase-2: Insight into the Formation of Products with Reversed Stereochemistry, Biochemistry 55(8) (2016) 1226–38. [PubMed: 26859324]

[49]. Roth GJ, Stanford N, Majerus PW, Acetylation of prostaglandin synthase by aspirin, Proc. Natl. Acad. Sci. U. S. A 72(8) (1975) 3073–6. [PubMed: 810797]

[50]. Kim SF, Huri DA, Snyder SH, Inducible nitric oxide synthase binds, S-nitrosylates, and activates cyclooxygenase-2, Science 310(5756) (2005) 1966–70. [PubMed: 16373578]

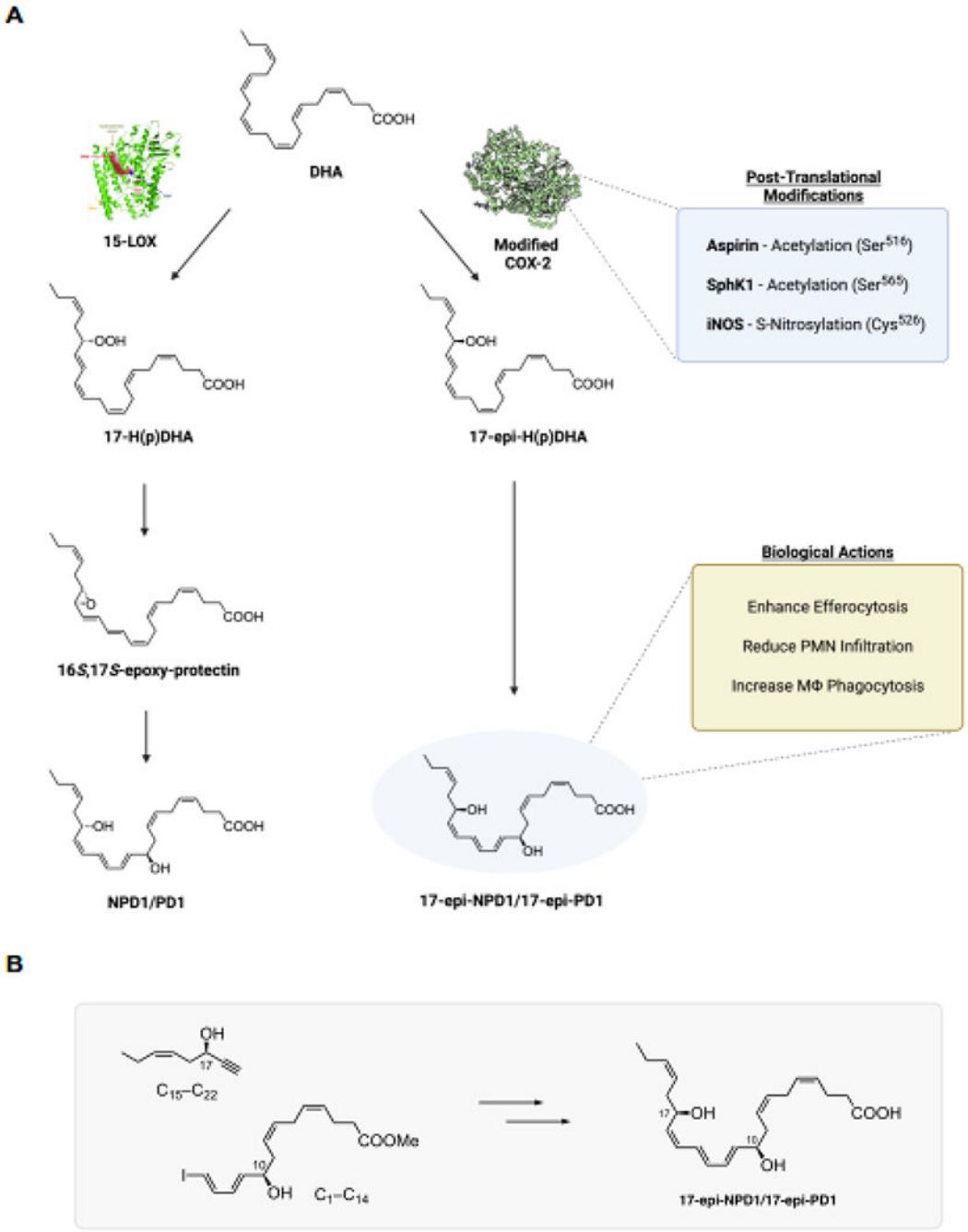

Figure 1. Illustration of 17-epi-NPD1/17-epi-PD1 proposed biosynthesis, actions, and synthetic strategy.

(A) Docosahexaenoic acid (DHA) is converted to 17*S*-H(p)DHA via 15-lipoxygenase to produce NPD1/PD1 [5, 8] via cell-type dependent pathways. For illustration, *in silico* *Pseudomonas aeruginosa*-derived 15-lipoxygenase crystal structure is shown docked with DHA from [47]. Also, DHA can be converted to 17*R*-H(p)DHA via the acetylation of COX-2 by aspirin (PDB 5F19, crystal structure from [48]. The 17*R*-hydroperoxide undergoes enzymatic epoxidation followed by enzymatic hydrolysis to 17-epi-NPD1/17-epi-

PD1; see [26]. COX-2 undergoes post-translational modifications that include acetylation and nitrosylation demonstrated in [27, 49, 50]. Figure illustration was created with Biorender.com. **(B)** A convergent synthetic approach of 17-epi-NPD1/17-epi-PD1 from two main precursors (see results section 3). Structures were made using ChemDraw level professional version 20.1.0.112 (PerkinElmer, Waltham, MA, USA).

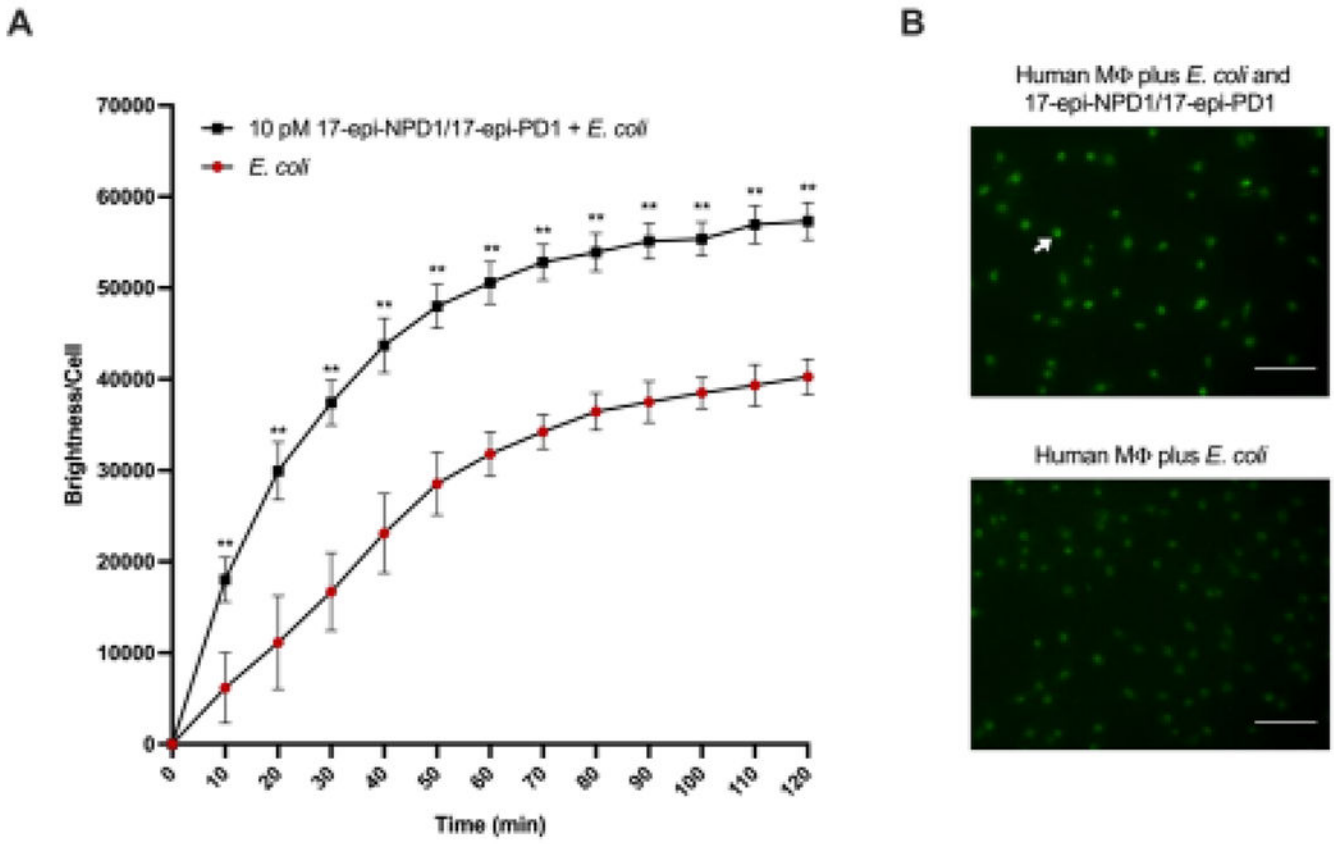

Figure 2. Human macrophages: 17-epi-NPD1/17-epi-PD1 enhances phagocytosis of bacteria.

(A) Real-time phagocytosis of *Bac*Light Green-labeled *E. coli* by human monocyte-derived macrophages (50 bacteria:1 macrophage ratio) in the presence of 10 pM 17-epi-NPD1/17-epi-PD1 or vehicle was monitored using fluorescence microscopy at 10-minute intervals for a total of 2 hours. Results are expressed as the mean brightness per macrophage. **(B)** Fluorescence microscopy of human macrophage phagocytosis in the presence or absence of 17-epi-NPD1/17-epi-PD1 (10 pM) following the addition of *E. coli* for 60 minutes. Representative images and the white arrow denote ingested bacteria and human macrophage. Scale bar represents 100 μm. These experiments were carried out in $PBS^{+/+}$ (pH 6.8-7.4), and the temperature was held at 37 °C in a thermal incubator (see Materials and Methods). n=4 individual donors; 4-5 fields were quantified per condition; error bars represent SEM. *, $P < 0.05$; **, $P < 0.01$ obtained with a two-tailed, paired Student's t-test for *E. coli* alone versus *E. coli* plus 17-epi-NPD1/17-epi-PD1.

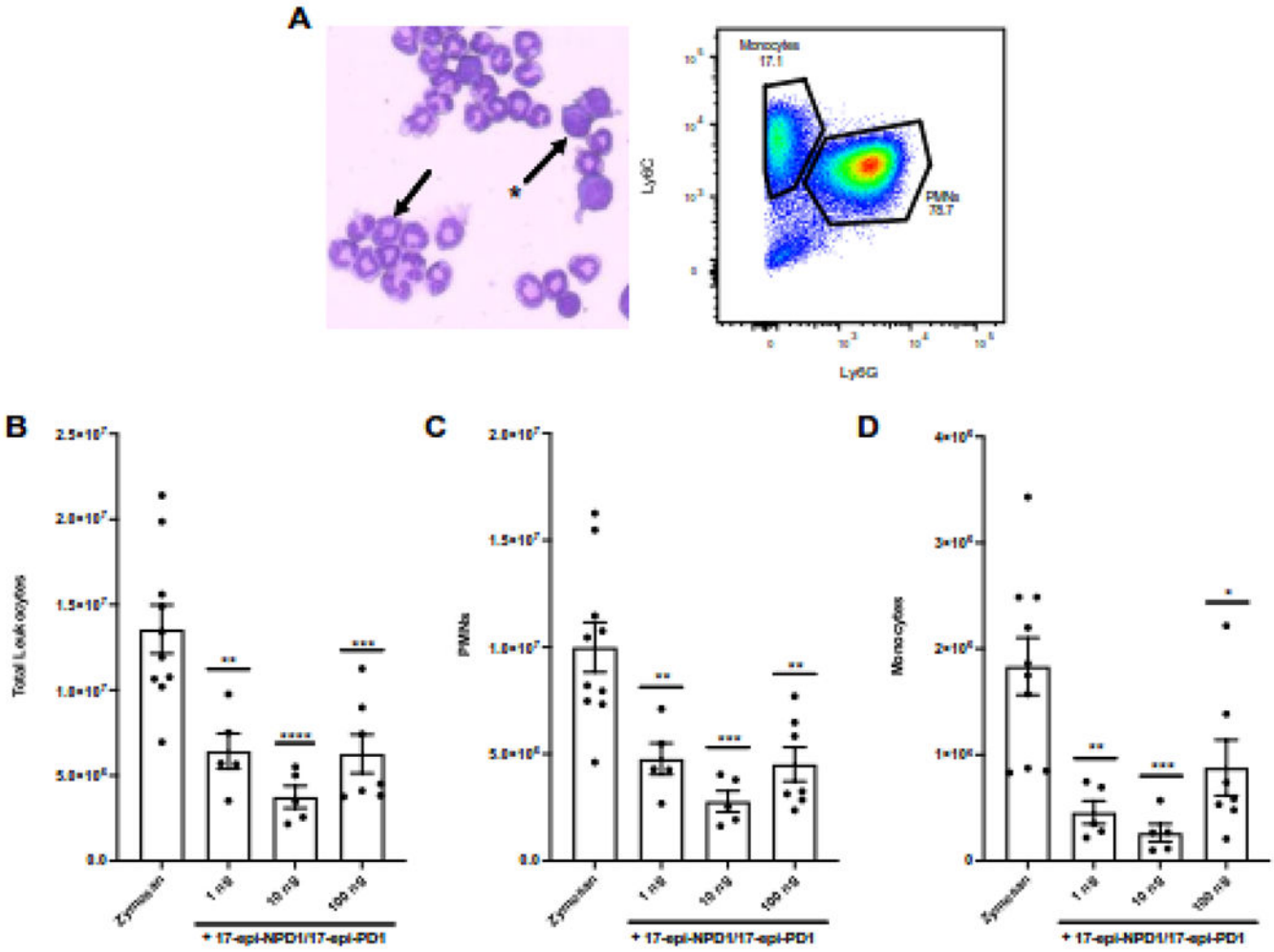

Figure 3. New synthetic 17-epi-NPD1/17-epi-PD1 limits PMN infiltration during peritonitis *in vivo*.

FVB mice were challenged i.p. with 2 mg zymosan immediately followed by i.v. delivery of vehicle (0.1% ethanol) or either 100 ng, 10 ng, or 1 ng of 17-epi-NPD1/17-epi-PD1 carboxy methyl ester in 100 μl of saline. Exudates were harvested via peritoneal lavage 6 hours later. **(A)** *Left,* A representative image of the exudate from a zymosan-challenged mouse stained with Wright-Giemsa. The arrow points to a polymorphonuclear cell; the star-arrow indicates a mononuclear cell. *Right*, A representative flow cytometry dot plot of the exudate of a zymosan-challenged mouse. **(B)** Total leukocyte counts were enumerated. **(C)** PMN ($CD45^+CD11b^+F4/80^-Ly6G^+$) numbers were determined using percentages obtained by flow cytometry. **(D)** Monocyte ($CD45^+CD11b^+F4/80^-Ly6C^+$) numbers were determined using percentages obtained by flow cytometry. Results are expressed as the mean ± SEM from two independent experiments, 5-10 mice total/group. *, $P < 0.05$; **, $P < 0.01$; ***, $P < 0.001$; ****, $P < 0.0001$ obtained with one-way ANOVA and Dunnett's multiple comparisons test for zymosan alone versus zymosan plus 17-epi-NPD1/17-epi-PD1.

A

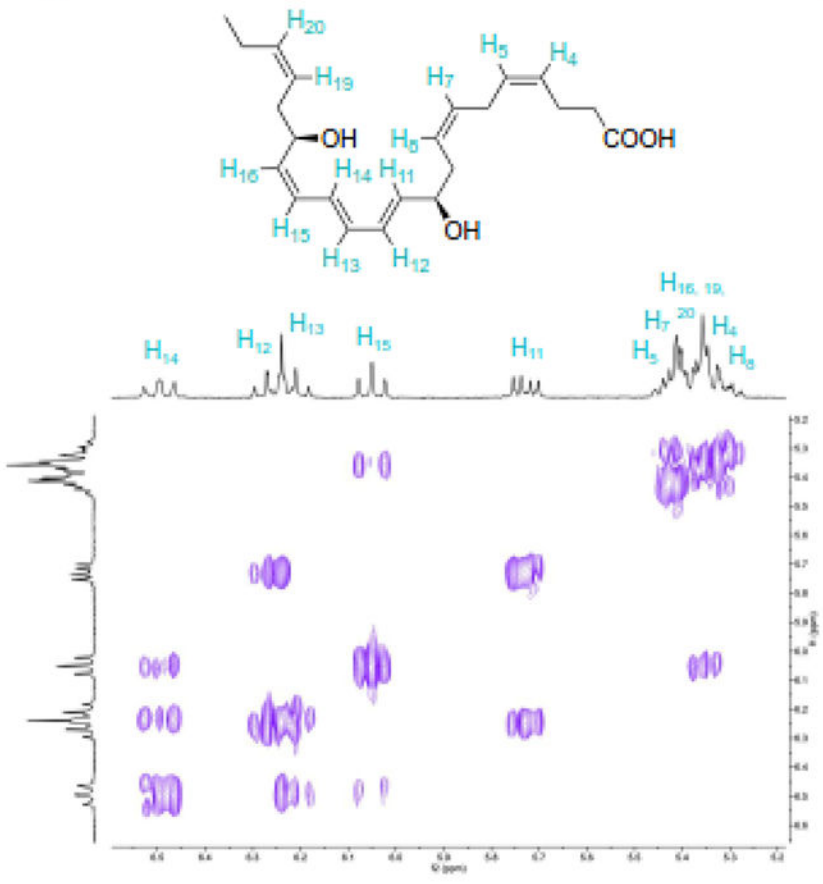

B

Position[a]	δH, mult. (J, Hz)[b]	COSY
1		
2	2.30 - 2.40, m	3
3	2.30 - 2.40, m	4
4	5.2 - 5.6, m	3, 5
5	5.2 - 5.6, m	6
6	2.7 - 2.9, m	5, 7
7	5.2 - 5.6, m	8
8	5.2 - 5.6, m	9
9	2.30 - 2.40, m	8, 10
10	4.1 - 4.2, m	9
11	5.75, dd (6.5, 14.5)	10, 12
12	6.2 - 6.4, m	11, 13
13	6.2 - 6.4, m	14
14	6.52, dd (12.1, 13.5)	13, 14
15	6.06, t (11.2)	14, 16
16	5.2 - 5.6, m	15, 17
17	4.5 - 4.6, m	16, 18
18	2.20 td (7.0, 14.1); 2.30 - 2.40, m	17, 18, 19
19	5.2 - 5.6, m	18
20	5.2 - 5.6, m	21
21	2.07, quin (7.3)	22
22	0.97, t (7.5)	21

[a]See Panel A for atom labelling. [b]Methanol-d_4 was used as solvent. Data procured at 400 MHz.

Figure 4. 2D COSY NMR of the newly synthesized 17-epi-NPD1/17-epi-PD1.

The total organic synthesis of 17-epi-NPD1/17-epi-PD1 was carried out and the product was taken for spectroscopic analysis. **(A)** Structure of 17-epi-NPD1/17-epi-PD1 highlighting alkenyl protons and 2D COSY NMR. **(B)** Full proton NMR data of 17-epi-NPD1/17-epi-PD1. These data were acquired using a JEOL ECZ-400S spectrometer equipped with a 5 mm ROYALPROBE™ HFX probe at 399.58 MFz for olefinic and full proton assignment.

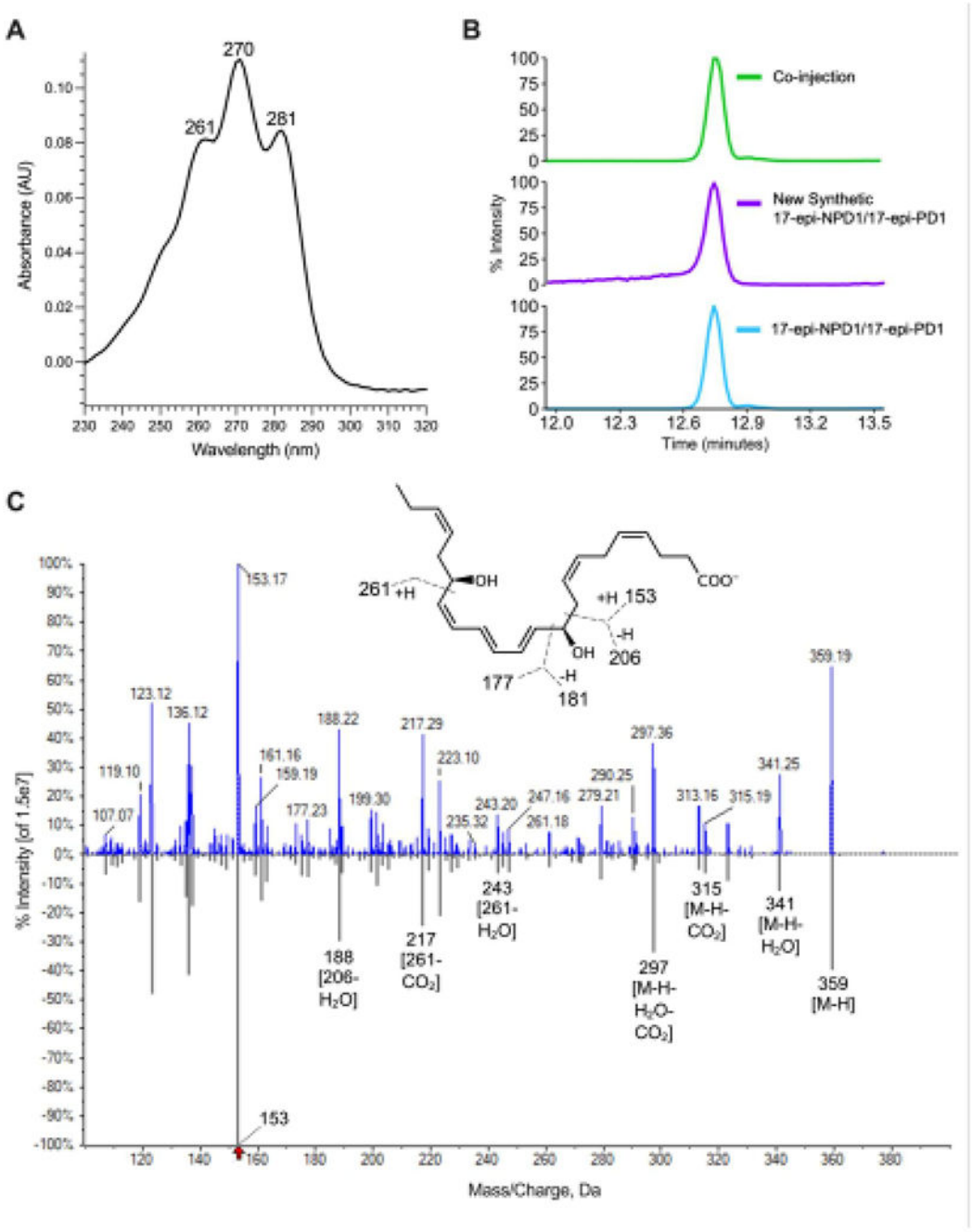

Figure 5. Matching authentication of the new synthetic 17-epi-NPD1/17-epi-PD1.

(A) UV absorption spectrum of new synthetic 17-epi-NPD1/17-epi-PD1 with a λ_{max}^{MeOH} at 270 nm and shoulders at 261 nm and 281 nm. **(B)** LC-MS/MS targeted MRM for *m/z* 359>153. The upper MRM is the co-injection of equal amounts (100 pg) of the newly synthesized and in-house reference 17-epi-NPD1/17-epi-PD1. **(C)** Enhanced product ion spectra with fragmentations of the new synthetic 17-epi-NPD1/17-epi-PD1 (99.6% library fit score). The upper fragmentations (blue) are from the new synthetic 17-epi-NPD1/17-epi-PD1, and the lower fragmentations (grey) are from the original 17-epi-NPD1/17-epi-PD1 in

a custom metabololipidomics library generated in LibraryView version 1.4 (Sciex). Please note, the accuracy for data acquisition of the Sciex 6500^{+} is 0.1 amu; the additional digits in this screen capture are the default settings. *Inset,* 17-epi-NPD1/17-epi-PD1 structure with proposed fragmentations.

Table 1.

Toxicity panel.

100 ng of 17-epi-NPD1/17-epi-PD1 methyl ester or vehicle (0.1% ethanol) were administered to mice i.v. in 100 μl of sterile saline, and blood was collected 24 hours later. Serum was analyzed for a panel of common toxicology markers and expressed as the mean ± SD of 3 mice per group. Unpaired, two-tailed *t* tests were performed for comparisons between vehicle control and 17-epi-NPD1/17-epi-PD1 for each analyte. ALP: alkaline phosphatase, AST: aspartate aminotransferase, ALT: alanine aminotransferase, ALB/GLOB: albumin/globulin, LDH: lactate dehydrogenase.

Analyte	Vehicle control (mean ± SD)	17-epi-NPD1/17-epi-PD1 (mean ± SD)	P-value
ALP (U/L)	147.00 ± 23.52	149.33 ± 2.89	0.8728
AST (U/L)	126.67 ± 57.55	177.00 ± 66.09	0.3761
ALT (U/L)	39.33 ± 11.01	70.67 ± 22.50	0.0962
Albumin (g/dL)	2.87 ± 0.12	2.83 ± 0.12	0.7415
Total bilirubin (mg/dL)	0.17 ± 0.06	0.23 ± 0.06	0.2302
Total protein (g/dL)	5.03 ± 0.21	5.00 ± 0.17	0.8416
Globulin (g/dL)	2.17 ± 0.15	2.17 ± 0.06	>0.9999
Bilirubin conjugated (mg/dL)	0.00 ± 0	0.00 ± 0	n/a
ALB/GLOB ratio (g/dL)	1.33 ± 0.12	1.30 ± 0	0.6433
LDH (U/L)	881.67 ± 34.65	1238.67 ± 383.32	0.1834
Bilirubin unconjugated (mg/dL)	0.17 ± 0.06	0.23 ± 0.06	0.2302